JOURNAL of the MEXICAN CHEMICAL SOCIETY

https://www.jmcs.org.mx/

Article

Open Access

J. Mex. Chem. Soc. **2026**, *70(1):e2426*

Received January 8th, 2025
Accepted June 16th, 2025

http://dx.doi.org/10.29356/jmcs.v70i1.2426
e-location ID: 2426

Keywords:
Natural dye, DSSC, cacti, photovoltaic response

Palabras clave:
Tinte natural, DSSC, cactus, respuesta fotovoltaica

***Corresponding author:**
Romero-Contreras A.
email: alfredoromcont@gmail.com

©2026, edited and distributed by Sociedad Química de México

ISSN-e 2594-0317

Exploring the Performance of Dye-Sensitized Solar Cells with *Escontria chiotilla* and *Stenocereus sp.* dyes

Romero-Contreras A.[1*], González-Juárez E.[1], Sandate-Flores L.[2], Sinagawa-García S.[3], De La Fuente-Loera R.[1], Sánchez-Cervantes E.[1]

[1]Facultad de Ciencias Químicas, Universidad Autónoma de Nuevo León, México.
[2]Tecnológico Nacional de México /ITS de Rioverde, México.
[3]Universidad Autónoma de Nuevo León, Facultad de Agronomía, UANL.

Abstract. In this study, natural dyes were extracted from two different cacti: *Stenocereus sp.* and *Escontria chiotilla peel*. The dyes were used as potential sensitizers for Dye-Sensitized Solar Cells (DSSCs). For *Stenocereus sp.* fruit, microfiltration and ultrafiltration processes were applied to obtain a purified sample and to investigate their effects on the photovoltaic response of DSSCs. The *Escontria chiotilla peel* extract was used directly. The chemical properties and stability of the dyes were investigated using UV-Vis spectroscopy, while FT-IR and XRD were used to identify the dye chemical composition and the structural features of working electrodes. Additionally, the photovoltaic properties of the fabricated devices were examined by measuring the J-V curves. It was found that the best performance was achieved using the *Escontria chiotilla* extract, yielding an efficiency of approximately 0.039 % due to the presence of chlorophyll as a sensitizer agent.

Resumen. En este estudio, se extrajeron colorantes naturales de dos distintos cactus: *Stenocereus sp*. y de *Escontria chiotilla*. Los colorantes se utilizaron como posibles colorantes para Celdas Solares Sensibilizadas por Tinte. Para el caso de *Stenocereus sp*, el extracto se sometió a procesos de microfiltración y ultrafiltración para obtener una muestra

©2026, Sociedad Química de México. Authors published within this journal retain copyright and grant the journal right of first publication with the work simultaneously licensed under a Creative Commons Attribution License that enables reusers to distribute, remix, adapt, and build upon the material in any medium or format for noncommercial purposes only, and only so long as attribution is given to the creator.

J. Mex. Chem. Soc. **2026**, *70(1):e2426*
Regular Issue
©2026, Sociedad Química de México
ISSN-e 2594-0317

purificada y posteriormente, investigar sus efectos en la respuesta fotovoltaica de las DSSC. El extracto de cáscara de *Escontria chiotilla* se utilizó directamente. Las propiedades químicas y la estabilidad de los tintes se investigaron mediante espectroscopia UV-Vis, mientras que las técnicas FT-IR y XRD se utilizaron para identificar la composición química de los tintes y la estructura de los electrodos de trabajo respectivamente. Adicionalmente, las propiedades fotovoltaicas de los dispositivos fabricados se examinaron midiendo las curvas J-V. Se encontró que el mejor rendimiento fue alcanzado utilizando el extracto de *Escontria chiotilla*, obteniéndose una eficiencia de aproximadamente 0.039 % debido a la presencia de clorofila como agente sensibilizador.

Introduction

Nowadays, renewable energy is gaining attention as a solution to the fossil energy crisis and the environmental problems associated with its excessive consumption [1,2]. As a promising energy source, solar radiation is one of the most abundant renewable energies and it is available worldwide. To harness solar radiation, several studies have focused their attention on generating electricity through low cost-effective devices such as Dye-Sensitized Solar Cells (DSSCs) [3-5]. These devices involve simple manufacturing processes with low production costs, and the resulting products are flexible, versatile in design, environmentally friendly, and exhibit efficiencies of around 13 % [6]. Essentially, DSSCs are composed of three parts: a counter-electrode, an electrolyte solution, and an electrode [7]. A typical electrode consists of a nanostructured semiconductor layer covered with a sensitizer, such as metal-based synthetic organic dyes. Devices with high-efficiency records typically use ruthenium polypyridyl complexes as effective sensitizers. However, ruthenium dyes are expensive, toxic, and require complex synthesis processes, leading to a negative environmental impact [8,9]. As an alternative, natural dyes emerged as possible sensitizers which are less expensive, environmentally friendly, non-toxic, easily extracted, readily available, and biodegradable [10,11]. These photosensitizers could be extracted from leaves [12], flowers [13], and fruits [14] and may contain anthocyanin, chlorophyll, carotenoid, and betalain molecules, which are suitable for anchoring to the semiconductor surface of the electrode and absorbing sunlight [15,16]. Recently, Erande and co-workers [17] extracted and evaluated a pomegranate fruit extract as a sensitizer. The fabricated devices sensitized with that dye, exhibited a maximum power conversion efficiency (PCE) of about 1.4 %. Risnah et al. [18] prepared an extract of eggplant skin and tested it as a natural dye for DSSCs. Their work showed that the sensitized devices achieved an efficiency of about 0.02 %. Taya and collaborators [19] worked on the extraction and sensitization of DSSCs using spinach, parsley, arugula, and green algae. They reported efficiencies of 0.29 %, 0.07 %, 0.2 %, and 0.01 %, respectively. Additionally, Ganta and co-workers [20] explored the use of two types of natural plant-based dyes extracted from cladode and the leaf of *Aloe vera*. The sensitized devices achieved efficiencies of 0.38 % and 0.74 %, respectively.

Alternatively, cacti have been explored as potential raw materials to extract natural dyes for their use in Dye-Sensitized Solar Cells for example, Obi et al., [21] demonstrated that extract from *Opuntia phaeacanth*a, a native cactus from North America, is viable as sensitizer since the fabricated devices achieved an efficiency close to 0.73 %. Moreover, Giron and coworkers analyzed the effectiveness of several natural dyes specially from a Mexican native cactus fruit named *Opuntia joconostle*, known as xoconostle, which contains betalain. The extracted dye was used in co-sensitization to achieve an efficiency of 0.0044 % [22]. Winston et al. tested several dyes for DSSCs applications, one of them was extracted from prickly pear, a cacti fruit which exhibited an efficiency around 0.4 %. [23]

In most cases, dyes are extracted from raw materials and used as prepared without further purification. Rarely, the extracts purification process is applied and the effects of those purified dyes on the performance of DSSCs are not explored. For example, Kabir et al. [24] used red spinach (*Amaranthus dubius*) as a sensitizer to enhance DSSC efficiency, achieving an efficiency of about 0.247 %. Furthermore, they refined the extract, and the filtered solution was used to sensibilize their electrodes. The results showed that efficiency increased by 2.7 times compared to that of the crude red spinach extract.

In this work, we explore the application of two natural pigments obtained from non-toxic cacti that can survive in dry conditions, are abundant in nature, and can be extracted using simple methods. These dyes were extracted from two fruits belonging to the Cactaceae family: *Stenocereus sp.* and *Escontria chiotilla* (known in

J. Mex. Chem. Soc. **2026**, *70(1):e2426*
Regular Issue
©2026, Sociedad Química de México
ISSN-e 2594-0317

Mexico as jiotilla). The dyes were characterized by UV–Vis absorption spectra and monitored over a month to verify their optical absorption stability. The photovoltaic properties of the fabricated DSSCs using these extracts as sensitizers were investigated by measuring the corresponding J-V curves. For the *Stenocereus sp*. extract, microfiltration and ultrafiltration processes were applied to extend our study of the effect of purification process on the device performance.

Experimental

Materials

For the synthesis of TiO_2 paste, absolute ethanol (CTR, >99 %), titanium dioxide (Sigma Aldrich, 99.5 %), acetic acid (sigma Aldrich, 99.9 %), terpineol (Sigma Aldrich, 96 %) and ethyl cellulose (Sigma Aldrich, 49 %wt.) were used without further purification. For the device fabrication, Fluorine doped tin oxide coated glass (FTO, surface resistivity ~8 Ω cm^{-2}), Hellmanex soap (laboratory grade), acetonitrile (Sigma-Aldrich, 99.9 %), tert-butyl alcohol (Sigma-Aldrich, 99.7 %) were used.

To prepare the counter electrodes, Chloroplatinic acid solution (8 % wt. in H2O) and isopropyl alcohol (98 %) were obtained from Sigma Aldrich. Finally, for the electrolyte solution preparation tetrapropylammonium iodide (98 %), iodide (99.8 %, solid) and methoxypropionitrile (98 %) were purchased from Sigma-Aldrich.

TiO_2 paste synthesis

To obtain the TiO_2 paste, 6 g of TiO_2 (Degussa, 99.5 %) were mixed with 1 mL of acetic acid in a mortar for 5 min. After that time, 1 mL of distilled water was added and mixed with the TiO_2 for 1 min. This step was repeated 5 times then 2.5 mL of ethanol was dropped into the paste and mixed for 1 min. To assure the viscosity of the paste, it was stirred using 100 mL of ethanol. During this process, 20 g of terpineol were mixed with the paste to finally add 3 g ethyl cellulose. The resultant sample was stirred and heated at 70 °C until it reached the optimal consistency.

Dye extraction

Escontria chiotilla fruits were harvested from a cultivated field in San Pedro Totolapam, Oaxaca, Mexico. *Escontria chiotilla* fruits were pre-treated by washing thoroughly with tap water and soap. The fruit peel was separated from the pulp and dried at 70 °C in an oven for 72 h. After that, the dried fruit peel was manually crushed and squeezed using a mortar and pestle. The solid fragments were soaked in 30 mL of 2:1 distilled water and ethyl alcohol mixture. Finally, the resultant dye was filtered and stored in the dark.

The *Stenocereus sp*. samples were obtained from a local establishment in Rioverde, San Luis Potosí, Mexico. The fruits were rinsed under running water at ambient temperature. The peel was then manually separated. The pulp was subsequently processed using an extractor to remove the seeds and centrifuged for 15 minutes at 4 °C at a speed of 6000 rpm. The centrifugation process (Z400K, Hermle, Germany; Centrifuge 5804 R, Eppendorf, Hamburg, Germany) was conducted using 50 mL Falcon tubes. The resulting supernatant from the centrifugation, referred to as clarified juice (CJ), was stored in darkness at 4 °C until further use.

The microfiltration and ultrafiltration procedures were carried out using a membrane filtration system designed by Membranology® (Swansea, UK). During microfiltration, the CJ was passed through a microfiltration cartridge filter (CFP-2-E-35A, GE Healthcare, Chicago, IL, USA) with a pore size of 0.2 μm. The resultant juice was labeled as MJ. After the microfiltration process, the ultrafiltration was conducted by passing the MF permeate through an ultrafiltration cartridge filter (UFP-10-C-5A, GE Healthcare) with a pore size of 10 kDa. The operating temperature was kept at 22 ± 2 °C. Finally, the resultant sample was stored in the dark and labeled as UJ (Ultrafiltered Juice). After extraction, all dye samples were kept at -10 °C to avoid decomposition. For its use in the sensitization process, dyes solutions were thawed in a water bath at 30 °C until the liquid phase was observed.

DSSCs fabrication

Electrodes fabrication

First, TiO_2 paste was deposited over an FTO (Fluorine-Tin Oxide) substrate by screen printing technique to obtain around 12 μm thick films. To evaporate out the solvents, TiO_2 films were kept in a muffle

http://dx.doi.org/10.29356/jmcs.v70i1.2426

J. Mex. Chem. Soc. **2026**, *70(1):e2426*
Regular Issue
©2026, Sociedad Química de México
ISSN-e 2594-0317

furnace at 500 °C for 0.5 h. After drying, the films were sensitized by separately soaking them in the natural dye solutions for 16 h.

Counter-electrodes fabrication

On the other hand, counter electrodes were fabricated by dropping a 0.3 M solution containing H_2PtC_{l6} dissolved in isopropyl alcohol over clean FTO substrates. After deposition, counter electrodes were dried at room temperature and finally were sintered at 450 °C in a furnace for 1h.

Electrolyte solution preparation

Electrolyte solution was prepared using a mixture of 0.5 M tetrapropylammonium iodine (TPAI) and 40 mM iodine dissolved in 3-methoxypropionitryle. The solution was stirred for 1 h at room temperature.

DSSCs assemble

After the sensitization process, the dye-coated film was rinsed with ethanol to remove unabsorbed dye and other remains which might be present on the surface. The electrode was set in a sandwich configuration with the counter-electrode. Both electrodes were assembled using binder clips by keeping electrical contacts on both sides. After that, electrolyte solution was allowed to diffuse in between the anode and the cathode, prior to taking the current-voltage curves.

Characterization

Betalain content determination

The betalain content was assessed by quantifying the levels of betacyanin (βC) and betaxanthins (βX) in the samples, according to the method described by Martínez et al. [25]. The extinction coefficients applied were E1% = 60,000 $Lmol^{-1}$ cm^{-1} at λ = 540 nm for βC, and E1% = 48,000 L mol^{-1} cm^{-1} at λ = 480 nm for βX. Results were expressed as the total concentration of βC and βX.

Structural and optical characterization

For X-ray diffraction, D2-Phaser, Bruker with Cu Kα radiation source (λ = 1.5418 Å) was used. The scanning rate was 0.05 °/s and analyzing within the angle range from 5 to 50°. UV-Vis spectra were recorded on an Evolution Pro UV-Vis spectrophotometer. Solutions of *Stenocereus sp*. extracts and *Escontria chiotilla* fruit were measured over a spectral range from 300 to 800 nm.

To measure the dye infrared spectra, pellets were prepared by using a drop of extracted dyes added to 300 mg KBr and mixed using a mortar to finally get a 1mm thickness pellet by using an 8 t press. The infrared spectrum was recorded at room temperature within a spectral range from 1000 to 3500 cm^{-1} with a 4 cm^{-1} resolution by using an Interspec 200-X FT-IR spectrometer.

Photovoltaic characterization

Current density-voltage (J-V) curves were studied using a Keithley-2400 sourcemeter unit under simulated irradiation by a 150 W Xe lamp with an intensity of 100 $mWcm^{-2}$. The applied voltage range was from 0 to 0.5 V. The fabricated devices were assembled with an effective area of 1.13 cm^2.

Results and discussion

Optical characterization

For photovoltaic applications, a dye with long-term stability is preferred. Usually, the stability of natural dyes decreases over time as they undergo biodegradation and photo-oxidation. Hence, the chemical stabilities of the natural dye samples extracted from *Stenocereus sp*. fruit and *Escontria chiotilla peels* in ethanol and distilled water were determined in the present research by UV-Vis measurements. The respective dye solutions were kept in the dark at room temperature, and their light absorbance intensities were periodically measured over 28 days (Fig. 1) except for clarified juice showed in Fig. 1**(b)**.

http://dx.doi.org/10.29356/jmcs.v70i1.2426

J. Mex. Chem. Soc. **2026**, *70(1):e2426*
Regular Issue
©2026, Sociedad Química de México
ISSN-e 2594-0317

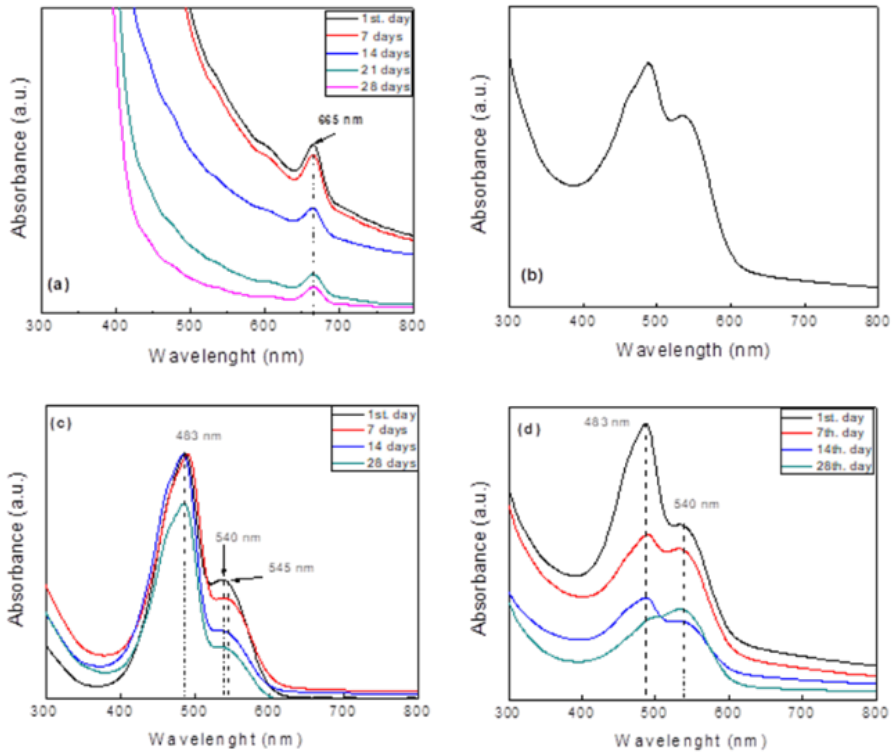

Fig. 1. UV-Vis analysis: **(a)** *Escontria chiotilla peel;* **(b)** clarified juice extracted from *Stenocereus sp*; **(c)**microfiltered juice (MJ); **(d)** Ultrafiltered juice (UJ).

Fig. 1**(a)** shows the spectra corresponding to the *Escontria chiotilla* peel extract. The peak observed at 665 nm corresponds to the absorption peak of chlorophyll A, which gives the characteristic green color to the peel and is related to the n to π* transition [26]. As shown, no shift in the peak was observed, indicating no chemical decomposition of chlorophyll over time which indicates the chemical stability of chlorophyll. Fig. 1**(b)** depicts the normalized absorption spectra for the clarified juice extracted from *Stenocereus sp*. Two characteristic peaks were observed at 480 and 540 nm revealing the presence of betaxanthin and betacyanin, respectively [27,28]. Fig. 1**(c)** depicts the absorption spectra for microfiltered juice (MJ). Two peaks were identified at 483 and 540 nm, which agree with the corresponding wavelengths for betaxanthin and betacyanin as observed for the clarified juice. For the first peak, the intensity decreases over time, indicating a decrease in the concentration of betaxanthins. A similar behavior was observed for the peak corresponding to the presence of betacyanin (540 nm), with the intensity decreasing over time and a slight shift to a longer wavelength. This shift may indicate the slight decomposition of betacyanin molecules after one week.

Finally, for the UJ sample, both peaks corresponding to betaxanthin and betacyanin were observed at their respective absorption wavelengths. The recorded signals showed a decrease in intensity over time, but no shift was observed until one month later. At this point, the peak at 483 nm (betaxanthin signal) shifted to a higher wavelength (492 nm), and its intensity decreased to a level lower than that of the peak at 540 nm, indicating the chemical decomposition of both molecules (Fig. 1**(d)**).

Structural characterization

Fig. 2 shows FT-IR spectra of *Stenocereus sp*. fruit extracts corresponding to the MJ and UJ samples diluted with ethanol and distilled water in a 1:1 proportion. First, the peak at 1100 cm^{-1} is related to the C-O stretching vibration. The peak located at 1409 cm^{-1} corresponds to the stretching of C-C in an aromatic group.

http://dx.doi.org/10.29356/jmcs.v70i1.2426

J. Mex. Chem. Soc. **2026**, *70(1):e2426*
Regular Issue
©2026, Sociedad Química de México
ISSN-e 2594-0317

The peak at 1623 cm^{-1} corresponds to the C=O stretching vibrations, which represent the carbonyl group in a ketone structure, and the broad peak at 3430 cm^{-1} is related to the N-H stretching vibration.

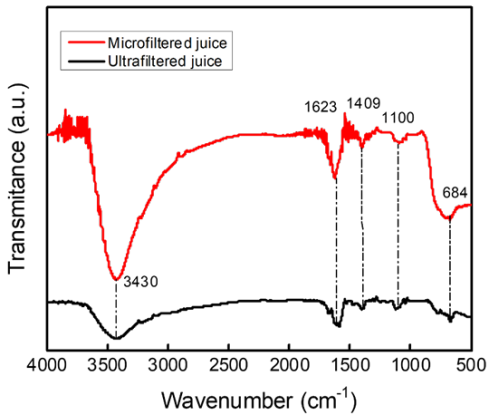

Fig. 2. FT-IR spectra of micro and ultrafiltered extracts from *Stenocereus sp* fruit.

When comparing the spectra, the same peaks appear in both samples, indicating that the method applied for the extraction of microfiltered and ultrafiltered samples does not modify the chemical structure of betacyanin and betaxanthin present in the *Stenocereus sp.* extracts [29,30].

In addition to their high absorption coefficient in the visible region of the electromagnetic spectrum, the presence of hydroxyl and carbonyl anchoring groups on betaxanthin and betacyanin enables their adsorption onto the surface of TiO_2. This adsorption facilitates the transfer of injected electrons from the dye to the conduction band of TiO_2, thereby enhancing the efficiency of DSSCs. Previous reports show how the dye anchors to the TiO_2 by describing the coupling between the energetic bands of both parts. From DFT simulations, it has been found that the HOMO and LUMO energies for betanin (betacyanin is a type of betanin) are -5.2 eV and -3.1 eV versus vacuum energy level, respectively [31]. These values estipulate that the band gap is about 2.1 eV which is in accordance with the calculated band gap obtained from the absorption peak of betacyanin (540 nm, band gap 2.2 eV). The DFT simulations provided information about the strong dipole–dipole interaction between the pigment and TiO_2 estimated in 8.69 Debye, which enables the good injection of electrons from the LUMO to the conduction band of the semiconductor, a diagram representing the alignment of the energy levels is represented in Fig. 3.

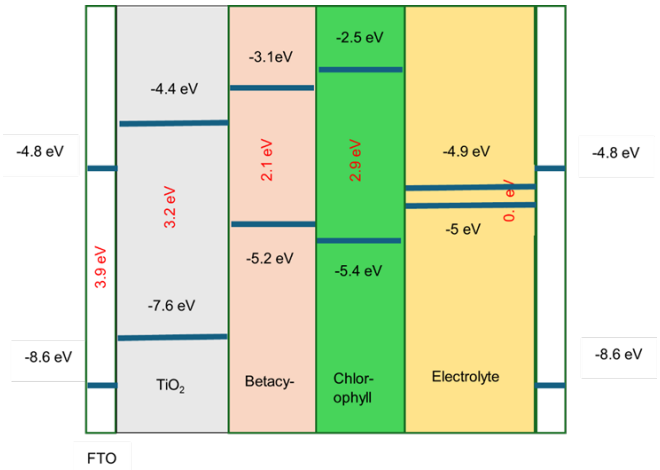

Fig. 3. Band diagram showing the alignment of energy levels (with respect to vacuum) of betacyanin and chlorophyll relative to the other components of a typical DSSC. The values corresponding to the band gaps are indicated in red. Data was obtained from [32,33]

http://dx.doi.org/10.29356/jmcs.v70i1.2426

J. Mex. Chem. Soc. **2026**, *70(1):e2426*
Regular Issue
©2026, Sociedad Química de México
ISSN-e 2594-0317

As described in the experimental section, a TiO_2 paste was prepared and characterized by X-ray diffraction (XRD). Fig. 4 presents the measured XRD pattern which is compared with the reported file COD number 7206075 [34]. The results provide evidence of the presence of anatase TiO_2 phase, as planes corresponding to the Miller indexes (1 0 1), (1 0 3), (0 0 4), (1 1 2), and (2 0 0) were identified. To verify the size of the synthetized particles, the Scherrer equation was applied and the results showed that the average crystallite size was about 12 ± 2.8 nanometers.

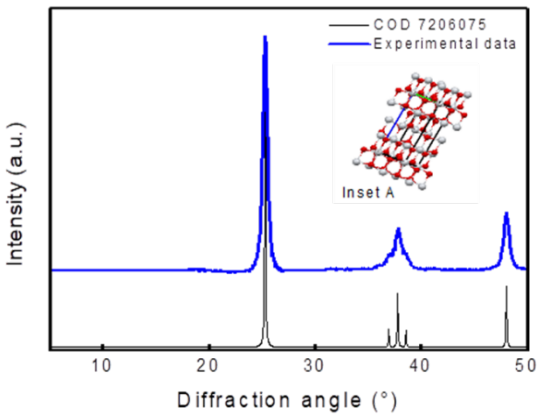

Fig. 4. XRD pattern corresponding to TiO_2 nanoparticles, the diffractogram is compared to the reported XRD pattern. Inset A shows a structural diagram of TiO_2, red spheres represent titanium atoms and grey spheres represent oxygen atoms.

Additionally, SEM images were taken at two different amplifications. Fig. 5(a) shows the image of TiO_2 nanoparticles at 25,000x, it is possible to distinguish the homogeneous distribution of nanoparticles and a rough surface also, a porous structure was observed. Moreover, Fig. 5(b) reveals that the nanoparticle size is below 100 nanometers in accordance with the calculation provided by Scherrer equation.

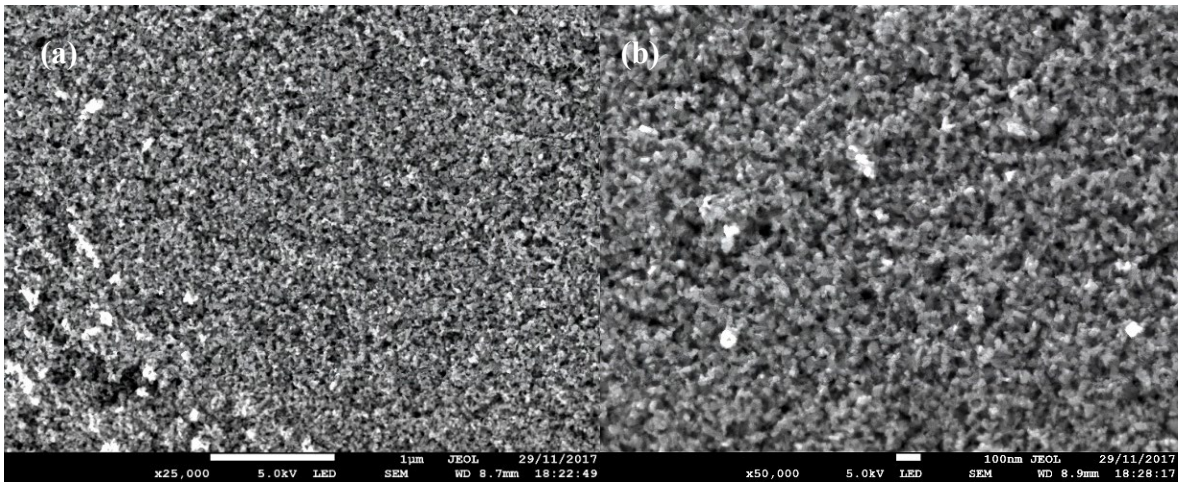

Fig. 5. SEM images of TiO_2 nanoparticles at **(a)** 25000x and **(b)** 50000x.

http://dx.doi.org/10.29356/jmcs.v70i1.2426

J. Mex. Chem. Soc. **2026**, *70(1):e2426*
Regular Issue
©2026, Sociedad Química de México
ISSN-e 2594-0317

Photovoltaic characterization

After the synthesis of TiO_2 nanoparticles, the fabrication of photovoltaic devices was carried out, and their performance as solar cells was analyzed through J-V curves. Fig. 6**(a)** depicts the representative J-V curves of devices sensitized with the natural extracts described in this manuscript. The photovoltaic parameters of the photoelectrodes were obtained under an illumination intensity of 100 mW cm^{-2} and an effective device area of 1.13 cm^2. As observed, the microfiltered juice showed better performance than the other samples from *Stenocereus sp.* fruit, even though the ultrafiltered juice achieved a higher current than the clarified juice. In Fig. 6**(b)**, we present the J-V curves corresponding to the best-performing *Stenocereus sp.* fruit extract and *Escontria chiotilla* extract for comparison. The voltages are similar for both devices, but *Escontria chiotilla* appears to achieve a slightly higher current density compared to the *Stenocereus sp*. extract.

The recorded average photovoltaic parameters related to *Escontria chiotilla* are summarized in Table 1. According to this table, the Power-Conversion Efficiency (PCE) for devices sensitized with *Escontria chiotilla* was close to 0.039 % with a short-circuit current of 0.15 mA cm^{-2} and an open-circuit voltage of 0.47 V. The standard deviation of reported values is relatively low, indicating no significant variations of the devices' performance.

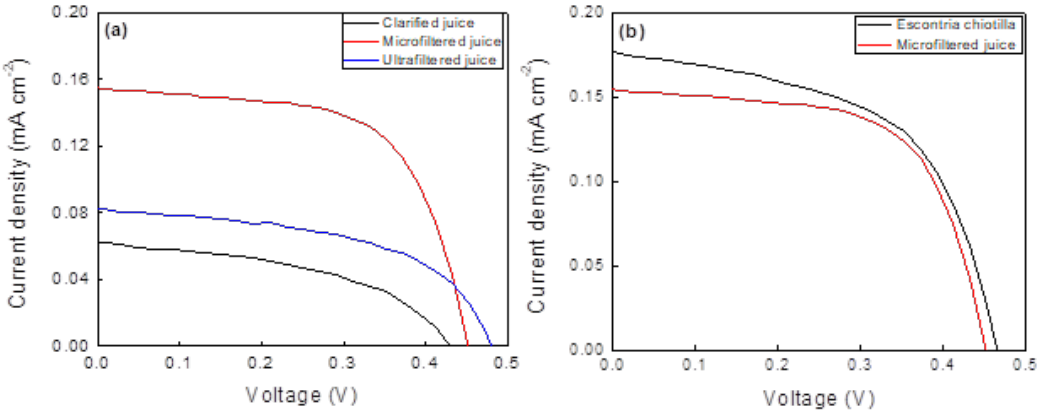

Fig. 6. (a) J-V curves corresponding to the *Stenocereus sp.* fruit extracts, **(b)** Curves for *Stenocereus sp*. microfiltered juice and *Escontria chiotilla* are graphed for comparison.

Table 1. Photovoltaic parameters for those devices sensitized with *Escontria chiotilla* extracts.

Parameter	Average	Standard deviation
PCE (%)	0.039	0.0058
FF (%)	55.62	5.198
Jsc (mA.cm^{-2})	0.15	0.0245
Voc (V)	0.47	0.0083

On the other hand, photovoltaic parameters for devices sensitized with CJ, MJ and UJ extracted from *Stenocereus sp* are listed in Table 2. PCE for these devices were 0.0142, 0.031 and 0.022 % respectively.

http://dx.doi.org/10.29356/jmcs.v70i1.2426

J. Mex. Chem. Soc. **2026**, *70(1):e2426*
Regular Issue
©2026, Sociedad Química de México
ISSN-e 2594-0317

Table 2. Photoconversion Efficiency and photovoltaic parameters extracted from J-V curves corresponding to the *Stenocereus sp* extracts.

Device label	PCE (%)	FF (%)	Jsc (mA cm^{-2})	Voc (V)
Clarified juice	0.0142	43.76	0.02	0.36
Microfiltered juice	0.031	46.12	0.06	0.31
Ultrafiltered juice	0.022	40.22	0.03	0.45

In accordance with the photovoltaic response exposed in Table 2, *Stenocereus sp.* fruit extracts reached the highest efficiency when it is subject to a microfiltered treatment mainly, the overall efficiency is influenced by the increase in the short-circuit current response.

To extend our understanding about the effect of filtration treatments, we carried out a quantitative phytochemical analysis which revealed the presence of phytochemicals, specifically betacyanin and betaxanthin; the concentrations for each sample are summarized in Table 3 and Table 4, respectively.

Table 3. Phytochemical analysis for betacyanin of *Stenocereus sp* fruit extracted in DI-water.

Betacyanin	Average concentration (mg L^{-1})	Standard deviation (mg L^{-1})
Clarified juice	228.31	23.66
Microfiltered juice	247.38	20.17
Ultrafiltered juice	122.71	3.86

Table 4. Phytochemical analysis for betaxanthins of *Stenocereus s*p extract in DI-water.

Betaxanthins	Average concentration (mg L^{-1})	Standard deviation (mg L^{-1})
Clarified juice	238.87	1.80
Microfiltered juice	250.68	0.59
Ultrafiltered juice	172.91	0.30

As shown in Table 3, extracts of *Stenocereus sp.* fruit contain varying amounts of betacyanin depending on the extraction procedure applied. The phytochemical analysis reveals that the betacyanin concentration is highest in the microfiltered sample compared to the clarified juice and ultrafiltered samples. Similarly, for betaxanthin concentration (Table 4), the microfiltered juice exhibits a higher concentration than the other samples.

A possible explanation is that betacyanin in raw materials is linked to a glucose molecule, typically referred to as glucosides. Glucosides consist of an aglycone (the dye molecule) and a glucose molecule. During the extraction of dye from the *Stenocereus sp.* peel, the glucose molecule remains intact, and no process is applied to prevent its interaction with betacyanin. During the sensitization of TiO_2, glucose molecules hinder full interaction between the anchoring groups in the betacyanin molecule and the TiO_2 surface, resulting in poor dye adsorption, fewer molecules available to absorb light, and a subsequent decrease in efficiency [35].

http://dx.doi.org/10.29356/jmcs.v70i1.2426

©2026, Sociedad Química de México
ISSN-e 2594-0317

However, when the microfiltration treatment is applied, glucose molecules may be separated from betacyanin, resulting in a microfiltered juice with a higher betacyanin concentration. This increases the number of dye molecules available to attach to the semiconductor surface, thereby improving the efficiency of the fabricated DSSC, as observed in our results. Conversely, the ultrafiltration procedure reduces the dye content in the microfiltered juice, resulting in an ultrafiltered juice with lower betacyanin concentration. Consequently, fewer dye molecules attach to the semiconductor surface, leading to reduced DSSC efficiency, as reflected in the photovoltaic parameters.

Conclusions

Dye extracts from *Stenocereus sp.* fruit and *Escontria chiotilla peels* were utilized as light-harvesting analogs in the fabrication of eco-friendly solar cells. This is the first time that *Escontria chiotilla* extract is reported as dye for DSSCs, and the first time that extract from *Stenocereus sp.* is put through a purification treatment and the resulting extracts are used as sensitizers. The chemical properties of studied dyes suggest that they cannot be used as sensitizers after one week since their optical properties decay after that time. On the other hand, structural, and photovoltaic properties of *Stenocereus sp*. and TiO_2-coated FTO glass were investigated via X-ray diffraction, UV-Vis spectroscopy and through J-V curves. The fabricated DSSC demonstrated the highest solar-to-electrical energy conversion efficiency with *Escontria chiotilla* as the sensitizer, achieving an average efficiency of approximately 0.039 %. Among the devices sensitized with *Stenocereus sp.* extracts, the best performance was obtained with the microfiltered juice, which yielded an efficiency of 0.031 %. Based on our results and previous reports, the performance of solar cells based on natural dyes is still less than compared with ruthenium-based dyes and further optimization is required.

Acknowledgements

Authors acknowledge to Secretaria de Ciencia, Humanidades, Tecnología e Innovación (Secihti), Mexico for financial support. A. Romero-Contreras acknowledges Secihti the invaluable opportunity granted through the postdoctoral fellowship 2023.

References

1. Rusilowati, U.; Ngemba, H. R.; Anugrah, R. W.; Fitriani, A.; Astuti, E. D. *Int. Trans. Artif. Intell.* **2024**, *2*, 114–120. DOI: https://doi.org/10.33050/italic.v2i2.537
2. Milani, S. J.; Bidhendi, G. N. *Water Sci. Eng.* **2023**, *17*, 283–291. DOI: https://doi.org/10.1016/j.wse.2023.11.003
3. Upadhyaya, H. M.; Senthilarasu, S.; Hsu, M.; Kumar, D. K. *Sol. Energy Mater. Sol. Cells.* **2013**, *119*, 291–295. DOI: https://doi.org/10.1016/j.solmat.2013.08.031
4. Devadiga, D.; Selvakumar, M.; Shetty, P.; Santosh. J. *Power Sources.* **2021**, *493*, 229698. DOI: https://doi.org/10.1016/j.jpowsour.2021.229698
5. Francis, O. I.; Ikenna, A. *Nat. Sci.* **2021**, *13*, 496–509. DOI: https://doi.org/10.4236/ns.2021.1312043
6. Best Research-Cell Efficiency Chart. Natl. Renewable Energy Lab. https://www.nrel.gov/pv/cell-efficiency.html, accessed in June 2025
7. Agrawal, A.; Siddiqui, S. A.; Soni, A.; Sharma, G. D. *Sol. Energy*. **2022**, *233*, 378–407. DOI: https://doi.org/10.1016/j.solener.2022.01.027
8. Buitrago, E.; Novello, A. M.; Meyer, T. *Helv. Chim. Acta.* **2020**, *103*. DOI: https://doi.org/10.1002/hlca.202000074

J. Mex. Chem. Soc. **2026**, *70(1):e2426*
Regular Issue
©2026, Sociedad Química de México
ISSN-e 2594-0317

9. Jitchati, R.; Thathong, Y.; Wongkhan, K. *Int. J. Appl. Phys. Math.* **2012**, *2*, 107–110. DOI: https://doi.org/10.7763/ijapm.2012.v2.64
10. Pramananda, V.; Fityay, T. A. H.; Misran, E. *IOP Conf. Ser.: Mater. Sci. Eng.* **2021**, *1122*, 012104. DOI: https://doi.org/10.1088/1757-899x/1122/1/012104
11. Ahmed, U.; Anwar, A., in: *Elsevier eBooks*; Elsevier: 2022, 45–73. DOI: https://doi.org/10.1016/b978-0-12-818206-2.00008-6
12. Taya, S. A.; El-Agez, T. A.; Elrefi, K. S.; Abdel-Latif, M. S. *Turk. J. Phys.* **2015**, *39*, 24–30. DOI: https://doi.org/10.3906/fiz-1312-12
13. Osolobri, B. U.; Enaroseha, O. E.; Anho, L. O. *Mater. Res. Innov.* **2024**, 1–8. DOI: https://doi.org/10.1080/14328917.2024.2389355
14. Kumaresan, S.; Subban, R.; Balasundaram, J. *Ionics*. **2024**. DOI: https://doi.org/10.1007/s11581-024-05771-3
15. Bist, A.; Chatterjee, S. *Energy Technol.* **2021**, *9*. DOI: https://doi.org/10.1002/ente.202001058
16. Dizama-Tzec, F. I.; García-Rodríguez, R.; Rodríguez-Gattorno, G.; Canto-Aguilar, E. J.; Vega-Poot, A. G.; Heredia-Cervera, B. E.; Villanueva-Cab, J.; Morales-Flores, N.; Pal, U.; Oskam, G. *RSC Adv.* **2016**, *6*, 37424–37433. DOI: https://doi.org/10.1039/c5ra25618f
17. Erande, K.; Hawaldar, P.; Suryawanshi, S.; Babar, B.; Mohite, A.; Shelke, H.; Nipane, S.; Pawar, U. *Mater. Today Proc.* **2021**, *43*, 2716–2720. DOI: https://doi.org/10.1016/j.matpr.2020.06.357
18. Risnah, I. A.; Aisyah, A.; Iswadi; Saokani, J. *Al-Kimia.* **2018**, *6*, 1–9. DOI: https://doi.org/10.24252/al-kimia.v6i1.4826
19. Taya, S. A. *Int. J. Mater. Sci. Appl.* **2013**, *2*, 37. DOI: https://doi.org/10.11648/j.ijmsa.20130202.11
20. Ganta, D.; Jara, J.; Villanueva, R. *Chem. Phys. Lett.* **2017**, *679*, 97–101. DOI: https://doi.org/10.1016/j.cplett.2017.04.094
21. Obi, K.; Frolova, L.; Fuierer, P. *Sol. Energy*. **2020**, *208*, 312–320. DOI: https://doi.org/10.1016/j.solener.2020.08.006
22. Girón-Juárez, K.; Messina-Fernández, S.; Navarro-Santos, P.; Vázquez-Guevara, M.; Mendoza-Pérez, J. *Optik.* **2024**, *306*, 171793. DOI: https://doi.org/10.1016/j.ijleo.2024.171793
23. Joseph, S.; Winston, A. J. P. P.; Muthupandi, S.; Shobha, P.; Margaret, S. M.; Sagayaraj, P. *J. Nanomater.* **2021**, *2021*, 1–12. DOI: https://doi.org/10.1155/2021/5540219
24. Kabir, F.; Bhuiyan, M. M. H.; Hossain, M. R.; Manir, M. S.; Rahaman, M. S.; Islam, M. T.; Ullah, S.M. *Optik* **2022**, *251*, 168452. DOI: https://doi.org/10.1016/j.ijleo.2021.168452
25. Martínez, E. M. M.; Sandate-Flores, L.; Rodríguez-Rodríguez, J.; Rostro-Alanis, M.; Parra-Arroyo, L.; Antunes-Ricardo, M.; Serna-Saldívar, S. O.; Iqbal, H. M. N.; Parra-Saldívar, R. *Plants*. **2021**, *10*, 368. DOI: https://doi.org/10.3390/plants10020368
26. Weiss, C. *Ann. N.Y. Acad. Sci.* **1975**, *244*, 204–213. DOI: https://doi.org/10.1111/j.1749-6632.1975.tb41532.x
27. Jahan, R.; Polash, M.; Karim, M.; Juthee, A.; Fakir, A.; Hossain, A. *Res. Crops*. **2021**, *22*. DOI: https://doi.org/10.31830/2348-7542.2021.060
28. Da Silva, D. V. T.; Baião, D. D. S.; Magalhães, A.; Almeida, N. F.; Conte, C. A.; Paschoalin, V. M. F. *Antioxidants.* **2023**, *12*, 1823. DOI: https://doi.org/10.3390/antiox12101823
29. Ghann, W.; Kang, H.; Sheikh, T.; Yadav, S.; Chavez-Gil, T.; Nesbitt, F.; Uddin, J. *Sci. Rep.* **2017**, *7*. DOI: https://doi.org/10.1038/srep41470
30. Rajaramanan, T.; Gourji, F. H.; Elilan, Y.; Yohi, S.; Senthilnanthanan, M.; Ravirajan, P.; Velauthapillai, D. *Sci. Rep.* **2023**, *13*. DOI: https://doi.org/10.1038/s41598-023-40437-6
31. Lopera, A.; Restrepo, J.; Vélez, E. *Adv. Theory Simul.* **2024**, *7*. DOI: https://doi.org/10.1002/adts.202400145
32. S, S.; Pesala, B. *ACS Omega*. **2019**, *4*, 18023–18034. DOI: https://doi.org/10.1021/acsomega.9b01875
33. Gonzalez-Flores, C. A.; Pourjafari, D.; Escalante, R.; Canto-Aguilar, E. J.; Poot, A. V.; Castán, J. M. A.; Kervella, Y.; Demadrille, R.; Riquelme, A. J.; Anta, J. A.; Oskam, G. *ACS Appl. Energy Mater.* **2022**, *5*, 14092–14106. DOI: https://doi.org/10.1021/acsaem.2c02609

J. Mex. Chem. Soc. **2026**, *70(1):e2426*
Regular Issue
©2026, Sociedad Química de México
ISSN-e 2594-0317

34. Rezaee, M.; Khoie, S. M. M.; Liu, K. H. *CrystEngComm*. **2011**, *13*, 5055. DOI: https://doi.org/10.1039/c1ce05185g
35. Gonçalves, L. C. P.; de Souza Trassi, M. A.; Lopes, N. B.; Dörr, F. A.; Santos, M. T. D.; Baader, W. J.; Oliveira, V. X.; Bastos, E. L. *Food Chem.* **2011**, *131*, 231–238. DOI: https://doi.org/10.1016/j.foodchem.2011.08.067